



Cite this: *Chem. Sci.*, 2023, **14**, 5768

All publication charges for this article have been paid for by the Royal Society of Chemistry

Received 1st February 2023  
Accepted 2nd May 2023

DOI: 10.1039/d3sc00556a  
[rsc.li/chemical-science](http://rsc.li/chemical-science)

## An AND-gate bioluminescent probe for precise tumor imaging†

Chenchen Wang,<sup>1</sup> Yajian Hong,<sup>a</sup> Ling Dong,<sup>b</sup> Hu Cheng,<sup>a</sup> Duo Jin,<sup>a</sup> Ronghua Zhao,<sup>c</sup> Zian Yu<sup>a</sup> and Yue Yuan <sup>\*a</sup>

Sensitivity and specificity are two indispensable requirements to ensure diagnostic accuracy. Dual-locked probes with "AND-gate" logic theory have emerged as a powerful tool to enhance imaging specificity, avoid "false positive" results, and realize correlation analysis. In addition, bioluminescence imaging (BLI) is an excitation-free optical modality with high sensitivity and low background and can thus be combined with a dual-locked strategy for precise disease imaging. Here, we developed a novel AND-gate bioluminescent probe, FK-Luc-BH, which is capable of responding to two different tumor biomarkers (cathepsin L and  $\text{ClO}^-$ ). The good specificity of FK-Luc-BH was proven, as an obvious BL signal could only be observed in the solution containing both cathepsin L (CTSL) and  $\text{ClO}^-$ . 4T1-fLuc cells and tumors treated with FK-Luc-BH exhibited significantly higher BL signals than those treated with unresponsive control compound Ac-Luc-EA or cotreated with FK-Luc-BH and a  $\text{ClO}^-$  scavenger/cathepsin inhibitor, demonstrating the ability of FK-Luc-BH to precisely recognize tumors in which CTS and  $\text{ClO}^-$  coexist.

## Introduction

Enhancement of diagnostic accuracy, including sensitivity and specificity, is of undoubtedly importance for clinical tumor imaging, especially early tumor diagnosis and imaging-guided surgery, to precisely delineate tumor margins in pre- and intra-operative realms and easily distinguish the tumor micro-environment from the surrounding normal tissues.<sup>1,2</sup> To realize tumor-specific imaging, many single-locked probes have been reported to enhance or suppress imaging signals at tumor sites after binding to or reacting with a specific biomarker, such as metal ions, proteinases, nucleic acids, membrane receptors, reactive oxygen species (ROS), and many other possible targets.<sup>3–9</sup> But sometimes, biomarkers that are overexpressed in tumors also exhibit considerable concentrations in other normal tissues, which may cause undesirable or even destructive "false-positive" diagnosis results.<sup>10</sup>

Inspired by the molecular logic gate reported by A. P. de Silva 29 years ago, multi-locked probes were proposed to regulate the imaging signal only when the simultaneous coexistence of two or more stimuli occurs, such as the "AND-gate" that is composed of

two or more inputs but only a single output.<sup>11</sup> Compared with a single-locked probe, the requirement of one more tumor-specific stimulus at the same site, *i.e.* a dual-locked probe, is capable of raising imaging accuracy, diminishing the misdiagnosis rate, and reflecting the interrelationship between two biomarkers in tumor development.<sup>12,13</sup> By changing the combination of biomarker-responsive sites, various dual-locked probes can be built for imaging different diseases or biological events.<sup>10</sup> An ideal dual-locked probe requires orthogonal responsive sites so that each biomarker can process only its corresponding responsive site.<sup>14,15</sup> Hence, employing a dual-locked probe to respond to two different types of biomarkers (such as one protease with one receptor or one ROS) was preferred to avoid cross reactions or their co-overexpression in normal tissues.

As a non-invasive biocompatible optical imaging modality, bioluminescence imaging (BLI) does not require an excitation source and thus has low background interference and an excellent signal-to-noise ratio (S/N).<sup>16</sup> Unlike complex fluorescent dyes for fluorescence imaging or photoacoustic imaging, the commonly used BLI probe amino-D-luciferin ( $\text{NH}_2\text{-Luc}$ ) is a small water-soluble molecule that is easy to synthesize and modify. Over the past few decades, almost all developed BL probes have been single-locked by simply caging their hydroxyl (amino) or carboxyl groups with stimuli-responsive motifs to block their recognition with luciferase and subsequent light emission.<sup>17</sup>

Herein, combining a specific dual-locked strategy and sensitive BLI modality, an AND-gate BL probe **FK-Luc-BH** with cathepsins and hypochlorite ( $\text{ClO}^-$ ) as two inputs was

<sup>a</sup>Department of Chemistry, University of Science and Technology of China, 96 Jinzhai Road, Hefei, Anhui 230026, China. E-mail: [yueyuan@ustc.edu.cn](mailto:yueyuan@ustc.edu.cn)

<sup>b</sup>Department of Chemistry and Chemical Engineering, Hefei Normal University, Hefei, Anhui 230061, China

<sup>c</sup>Center for Biomedical Imaging, University of Science and Technology of China, Hefei, Anhui 230026, China

† Electronic supplementary information (ESI) available. See DOI: <https://doi.org/10.1039/d3sc00556a>



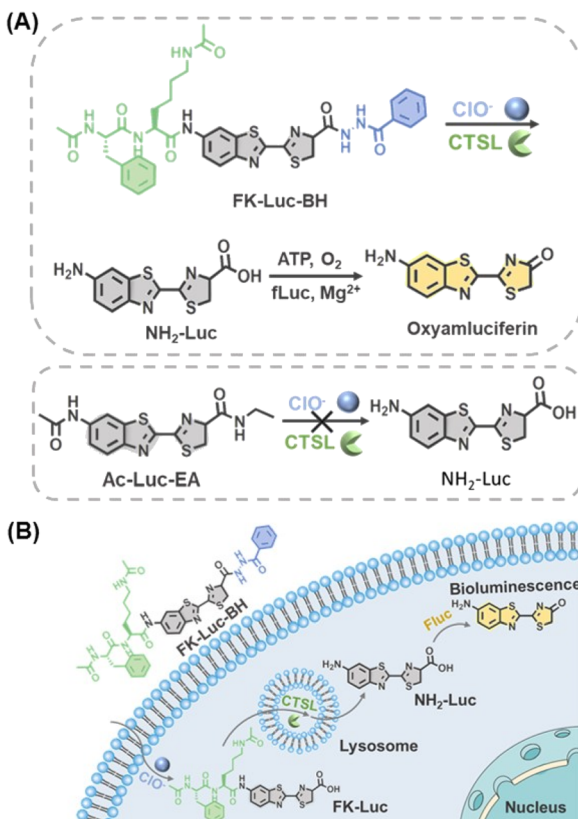


Fig. 1 (A) Chemical structure and (B) schematic illustration of an AND-gate bioluminescent probe for simultaneous monitoring of cathepsins and  $\text{ClO}^-$  in tumor cells.

constructed to realize accurate tumor imaging. Cathepsins belong to the papain subfamily of cysteine proteases and were reported as potential malignant tumor biomarkers; their over-expression is related to various types of cancers.<sup>18</sup> Hypochlorite ( $\text{ClO}^-$ ) is a member of the ROS family that is overproduced in many disorders and diseases, including cancer and inflammation.<sup>19-22</sup> The levels of both cathepsins and  $\text{ClO}^-$  are significantly increased in the early stage of malignant tumors, which enables their corresponding biosensors to distinguish early-stage tumors and small metastases from surrounding normal tissues.<sup>23,24</sup> After caging the amino group of NH<sub>2</sub>-Luc with a cathepsin-recognized substrate Phe-Lys (FK, mainly for cathepsin L in this work) and the carboxyl group of NH<sub>2</sub>-Luc with  $\text{ClO}^-$  reactive motif benzoylhydrazine, a dual-locked BLI probe **FK-Luc-BH** was produced for the following tumor-targeted imaging (Fig. 1A). When the probe **FK-Luc-BH** enters tumor cells that co-express cathepsin L (CTSL) and  $\text{ClO}^-$ , both peptide FK and benzoylhydrazine are removed to yield NH<sub>2</sub>-Luc, which reacts with firefly luciferase (fLuc), Mg<sup>2+</sup>, O<sub>2</sub>, and adenosine triphosphate (ATP) to emit a bright BL signal to precisely illuminate the tumor (Fig. 1B).

## Results and discussion

Before investigating the ability of **FK-Luc-BH** to react with cathepsins, **FK-Luc** was prepared to compare the enzymatic

efficiencies of cathepsin B (CTSB) and CTS-L, as both of them were reported to be capable of cleaving dipeptide FK (Scheme S1 and Fig. S1-S6†).<sup>2,25</sup> Then a series of concentrations of CTSB (0.0–8.0 U/L) or CTS-L (0.0–1.6 U/L) were incubated with 25  $\mu\text{M}$  **FK-Luc** in working buffer at 37 °C for 2 h, and the BL intensities were measured after adding 0.1 mg mL<sup>-1</sup> fLuc, 1 mM ATP, and 10 mM Mg<sup>2+</sup> (Fig. S7A and S8A†). As shown in Fig. S7B and S8B†, a good linear relationship between the BL intensity at 595 nm and the concentration of CTSB ( $Y = 13.38 + 63.57X$ ,  $R^2 = 0.9950$ ) or CTS-L ( $Y = 10.01 + 483.2X$ ,  $R^2 = 0.9913$ ) was obtained, and the limit of detection (LOD) of **FK-Luc** toward CTSB was calculated to be 0.03850 U/L (S/N = 3), which is about 7.0-fold higher than that for CTS-L (0.005536 U/L, S/N = 3), indicating that the dipeptide FK was more sensitive to the CTS-L response. Hence, the following *in vitro* experiments were mainly performed with CTS-L. Furthermore, we synthesized a control probe **Luc-BH** with reactive motif benzoylhydrazine for  $\text{ClO}^-$  detection (Scheme S2, Fig. S9 and S10†). After incubating different concentrations of  $\text{ClO}^-$  with 25  $\mu\text{M}$  of **Luc-BH** for 2 h at 37 °C, the BL intensity of **Luc-BH** at 595 nm was found to have a good linear relationship ( $Y = 0.8241X - 3.831$ ,  $R^2 = 0.9972$ ) with the concentration of  $\text{ClO}^-$  ranging from 10 to 80  $\mu\text{M}$  (Fig. S11†), and the LOD of  $\text{ClO}^-$  was calculated to be 0.8613  $\mu\text{M}$  (S/N = 3). These results demonstrated the feasibility of the probe with a benzoylhydrazine structure for the  $\text{ClO}^-$  response.

The detailed synthetic procedures and characterization studies of **FK-Luc-BH** are shown in Scheme S3 and Fig. S12–S14,† including its <sup>1</sup>H and <sup>13</sup>C nuclear magnetic resonance (NMR) spectroscopy spectrum and mass spectrum (MS). After incubating 25  $\mu\text{M}$  **FK-Luc-BH** with 2 U/L CTS-L or 1 mM  $\text{ClO}^-$  in CTS-L working buffer at 37 °C for 4 h, the high-performance liquid chromatography (HPLC) assay combined with the MS results verified that **Luc-BH** (olive line in Fig. 2A, S15, S16, and Table S1†) was produced as a result of the enzymatic cleavage of peptide FK on probe **FK-Luc-BH** by CTS-L, and **FK-Luc** was generated after oxidation of the benzoylhydrazine by  $\text{ClO}^-$  (blue line in Fig. 2A, S15 and S17†). As predicted, **FK-Luc-BH** was able to convert to free NH<sub>2</sub>-Luc for BL imaging under the co-incubation of CTS-L and  $\text{ClO}^-$  (red line in Fig. 2A, S15 and S18†). Then we studied the BL properties of **FK-Luc-BH** after treatment with only CTS-L, only  $\text{ClO}^-$ , and both, respectively. As shown in Fig. 2B, when 25  $\mu\text{M}$  **FK-Luc-BH** was co-incubated with both 2 U/L CTS-L and 200  $\mu\text{M}$   $\text{ClO}^-$  at 37 °C for 2 h, a clear BL signal could be observed after adding 0.1 mg mL<sup>-1</sup> fLuc, 1 mM ATP, and 10 mM Mg<sup>2+</sup>, resulting from the generation of the fLuc substrate NH<sub>2</sub>-Luc (Fig. 1A). In contrast, in the absence of either CTS-L or  $\text{ClO}^-$ , their BL intensities after the addition of fLuc were as weak as that of untreated **FK-Luc-BH** (Fig. 2B), indicating that **FK-Luc-BH** could only be efficiently activated for BL imaging with the coexistence of both CTS-L and  $\text{ClO}^-$ . Then the reaction of **FK-Luc-BH** with  $\text{ClO}^-$  was observed to follow second order kinetics with a rate constant of 0.3009  $\text{M}^{-1} \text{min}^{-1}$  (Fig. S19†). The kinetic parameters of CTSB/CTSL toward probe **FK-Luc-BH** were investigated according to the Michaelis-Menten equation. As displayed in Fig. S20 and S21,† the calculated catalytic efficiency ( $k_{\text{cat}}/K_m$ ) of CTS-L (4.376  $\mu\text{M}^{-1} \text{min}^{-1}$ ) is about 1 order of magnitude larger than that of

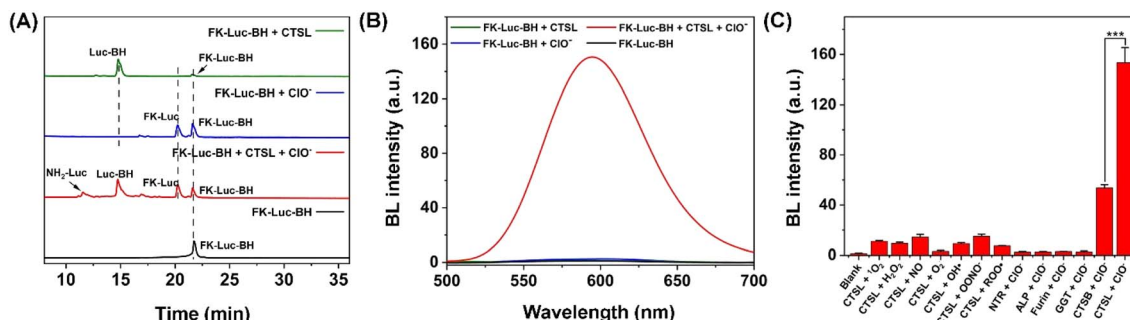


Fig. 2 (A) HPLC traces of 25  $\mu$ M FK-Luc-BH (blank) or 25  $\mu$ M FK-Luc-BH in the presence of 2 U/L CTS (olive), 1 mM  $\text{ClO}^-$  (blue), and 2 U/L CTS (red) in CTS working buffer (400 mM  $\text{CH}_3\text{COONa}$ , 4 mM EDTA, 2 mM GSH, 10% DMSO, pH = 7.0) for 4 h, respectively. (B) BL spectra of 25  $\mu$ M FK-Luc-BH (blank) or 25  $\mu$ M FK-Luc-BH in the presence of 2 U/L CTS together with 200  $\mu$ M  $\text{ClO}^-$  (red), 200  $\mu$ M  $\text{ClO}^-$  only (blue), and 2 U/L CTS only (olive) in the CTS working buffer for 2 h, respectively. (C) Selectivity of 25  $\mu$ M FK-Luc-ClO against potential interfering stimulus pairs. Concentrations for incubation: 200  $\mu$ M  $\text{O}_2^-$ , 200  $\mu$ M  $\text{H}_2\text{O}_2$ , 200  $\mu$ M NO, 200  $\mu$ M  $\text{O}_2^-$ , 200  $\mu$ M  $\text{OH}^-$ , 200  $\mu$ M  $\text{ONOO}^-$ , 200  $\mu$ M  $\text{ROO}^-$ , 200  $\mu$ M  $\text{ClO}^-$ , 2 U/L CTS, 2 U/L CTS, 100 U/L NTR, 100 U/L ALP, 100 U/L furin, and 100 U/L GGT. Error bars represent the standard deviations of three independent experiments, and the *p* value was obtained from *t*-tests using comparisons of two groups (\*\* for *p* = 0.0002).

CTSB ( $0.3412 \mu\text{M}^{-1} \text{min}^{-1}$ ), further suggesting that **FK-Luc-BH** was much more sensitive to CTS than to CTSB.

To confirm the specificity of **FK-Luc-BH** for imaging tumor cells co-overexpressing both CTS and  $\text{ClO}^-$ , the selectivity of **FK-Luc-BH** was assessed over a series of biological species that widely occur in living cells. After the addition of fLuc, ATP, and  $\text{Mg}^{2+}$ , no obvious BL signals were noticed when **FK-Luc-BH** was incubated with different types of ROS and nitrogen species (RNS), *e.g.*, nitric oxide (NO), hydrogen peroxide ( $\text{H}_2\text{O}_2$ ), hydroxyl radical ( $\text{OH}^-$ ), peroxynitrite ( $\text{ONOO}^-$ ), peroxy radical ( $\text{ROO}^\cdot$ ), superoxide anion ( $\text{O}_2^-$ ), singlet oxygen ( $\text{O}_2^\cdot$ ), and  $\text{ClO}^-$ , as well as intracellular abundant reduced glutathione (GSH) and common cancer cell-overexpressing enzymes including nitroreductase (NTR), alkaline phosphatase (ALP), furin,  $\gamma$ -glutamyltranspeptidase (GGT), and CTSB, respectively ( $37^\circ\text{C}$ , 2 h).<sup>26-29</sup> Remarkable enhancements in BL intensity were only observed when incubating **FK-Luc-BH** simultaneously with 200  $\mu$ M  $\text{ClO}^-$  and 2 U/L CTS/CTSB, and CTS triggered significantly higher intensity than CTSB (Fig. S22†). To further confirm the specificity of **FK-Luc-BH** toward cathepsins with  $\text{ClO}^-$ , the selectivity of **FK-Luc-BH** against various potential interfering stimulus pairs was tested respectively. As displayed in Fig. 2C, the BL intensity changes were evident only in the copresence of CTSB/CTSL with  $\text{ClO}^-$ , indicating that **FK-Luc-BH** shows rather better selectivity towards cathepsins +  $\text{ClO}^-$  compared with other potential intracellular interfering stimulus pairs and is thus able to accurately identify cathepsin and  $\text{ClO}^-$  co-abundant environments.

To prove that the BL signal of **FK-Luc-BH** was indeed mediated by cathepsins and  $\text{ClO}^-$ , a control compound **Ac-Luc-EA** was constructed with an acetyl group *in lieu* of the CTS substrate FK and benzoylhydrazine was replaced by ethylamine; hence, it cannot be cleaved by CTS and oxidized by  $\text{ClO}^-$  to expose  $\text{NH}_2\text{-Luc}$  for BLI (Fig. S23–S26†). The cytotoxicities of **FK-Luc-BH** and the control compound **Ac-Luc-EA** were studied on CTSL-overexpressed 4T1 mouse mammary tumor cells by the 3-(4,5-dimethylthiazol-2-yl)-2,5-diphenyltetrazolium bromide (MTT) assay (Fig. S27 and S28†). High survival rates of the 4T1

cells were obtained after treatment with 12.5  $\mu$ M, 25  $\mu$ M, and 50  $\mu$ M **FK-Luc-BH** or **Ac-Luc-EA** for 48 h, respectively, suggesting their good biocompatibility (Fig. S29†).<sup>30</sup> Then the BL signals were dynamically monitored after incubating fLuc-transfected 4T1 cells (4T1-fLuc) with 25  $\mu$ M **FK-Luc-BH** or 25  $\mu$ M control compound **Ac-Luc-EA**. The signal intensity of **FK-Luc-BH** treated cells gradually increased to their maximum at 90 min after an initial rapid increase from 5 min to 30 min and could still be detected at 210 min post-incubation, demonstrating that endogenous  $\text{ClO}^-$  and CTS could trigger **FK-Luc-BH** to yield free  $\text{NH}_2\text{-Luc}$  for BL “on”. The **Ac-Luc-EA** incubated cells, by contrast, exhibited very weak BL signals all through 5 min to 210 min, because the fLuc substrate was incapable of being activated in 4T1 cells (Fig. 3). To further confirm that the activation of **FK-Luc-BH** was induced by  $\text{ClO}^-$  and CTS, 4T1-fLuc cells were preincubated with 250 mM  $\text{ClO}^-$  scavenger taurine for 5 min, 500  $\mu$ M E-64d for 30 min, and 500  $\mu$ M E-64d for 25 min together with 250 mM taurine for another 5 min (the incubation time of E-64d is 30 min in total), respectively. The time courses of the BL signal after incubation with 25  $\mu$ M **FK-Luc-BH** showed that all their BL signal intensities were very weak from 5 min to 210 min and significantly lower than those of **FK-Luc-BH** treated fLuc-transfected 4T1 cells, which further proves that **FK-Luc-BH** is indeed a dual-locked AND-gate BL probe for tumor cell imaging, as its illumination specifically requires both  $\text{ClO}^-$  and CTS (Fig. 3 and S30†).

Finally, the capability of **FK-Luc-BH** to detect the coexistence of cathepsins and  $\text{ClO}^-$  *in vivo* for precise tumor diagnosis was evaluated.  $3 \times 10^5$  4T1-fLuc cells were implanted into the mammary fat pads of 7-week-old Balb/c mice to generate an orthotopic mouse model of breast cancer. After 7 days, the tumor-bearing Balb/c mice were randomly divided into five groups (*n* = 3 for each group): mice in the experimental group **FK-Luc-BH** or the control group **Ac-Luc-EA** were injected intraperitoneally (i.p.) with **FK-Luc-BH** or **Ac-Luc-EA** (12.5  $\mu$ mol  $\text{kg}^{-1}$ ); mice in the control groups taurine + **FK-Luc-BH**, E-64d + **FK-Luc-BH**, and taurine + E-64d + **FK-Luc-BH** were pre-injected i.p. with 3 mmol  $\text{kg}^{-1}$  taurine for 5 min, 0.05 mmol  $\text{kg}^{-1}$  E-64d

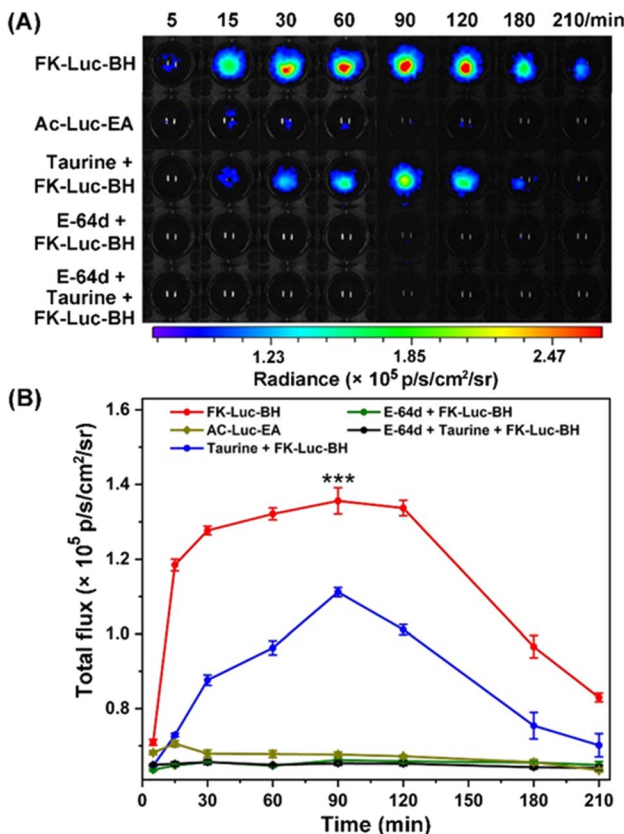
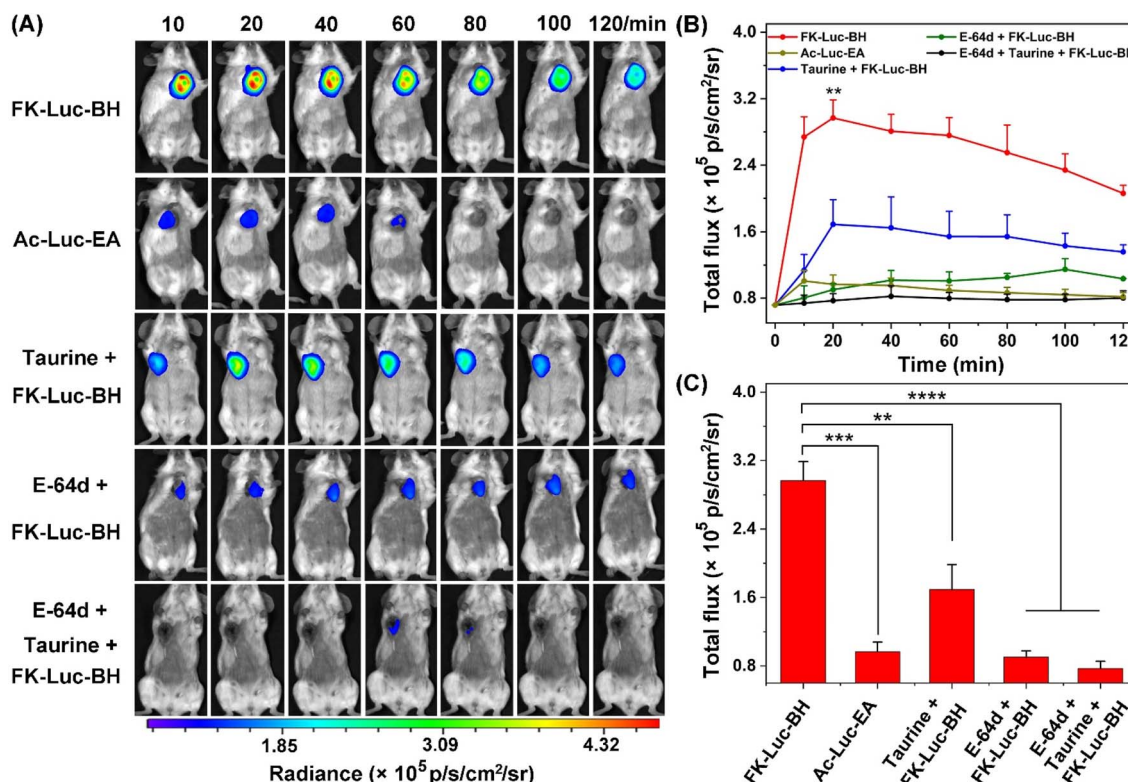


Fig. 3 (A) Time-course BL images of 4T1-fLuc cells after incubating with 25  $\mu$ M FK-Luc-BH, 25  $\mu$ M control compound Ac-Luc-EA, and 25  $\mu$ M FK-Luc-BH after pretreatment with 250 mM  $\text{ClO}^-$  scavenger taurine for 5 min, 500  $\mu$ M broad-spectrum cathepsin inhibitor E-64d for 30 min, or both of them, respectively. The images were acquired at 5, 15, 30, 60, 90, 120, 180, and 210 min post-incubation. The cells were placed in cell culture medium at 37 °C. All BL images reflect representative data from *in vitro* experiments repeated three times. (B) Quantified total photon output of (A) using ImageJ software. Each error bar represents the standard deviation of three independent experiments; the *p* value was obtained from *t*-tests using comparisons of the FK-Luc-BH group and taurine + FK-Luc-BH group (\*\*\* for *p* = 0.0003).

for 1 h, and 0.05 mmol kg<sup>-1</sup> E-64d for 55 min together with 3 mmol kg<sup>-1</sup> taurine for another 5 min, respectively, followed by the intraperitoneal administration of **FK-Luc-BH** (12.5  $\mu$ mol kg<sup>-1</sup>). For each group, time-course BL images of the breast tumor-bearing Balb/c mice were acquired from 10 to 120 min after the injection of **FK-Luc-BH**. As shown in Fig. 4, the BL intensity from the 4T1-fLuc tumors in the **FK-Luc-BH** group (the top row) obviously increased post-injection and reached its peak at 20 min; over 59% of the BL signal remained even at 120 min after injection, suggesting that **FK-Luc-BH** could quickly respond to  $\text{ClO}^-$  and CTS, accompanied by producing  $\text{NH}_2\text{-Luc}$  for BL generation. In comparison, the BL signal from the control group **Ac-Luc-EA** was much lower at 20 min and difficult to observe at 80 min post-injection, resulting from its unresponsive molecular structure. For the other three control groups taurine + **FK-Luc-BH**, E-64d + **FK-Luc-BH**, and taurine + E-64d + **FK-Luc-BH**, the expression level of either  $\text{ClO}^-$  or CTS was

reduced, and the BL signals of the tumors were significantly lower than those of the **FK-Luc-BH** group during the observation period. The quantitative results showed that the BL intensities of the taurine + **FK-Luc-BH** group, E-64d + **FK-Luc-BH** group, and E-64d + taurine + **FK-Luc-BH** group were 1.76-, 3.29-, and 3.86-fold lower than that of the **FK-Luc-BH** group at 20 min, respectively. These results demonstrated that **FK-Luc-BH** could be employed for sensitively and efficiently imaging tumor cells co-expressing  $\text{ClO}^-$  and CTS. Similar to the above cell experiment results, among all the control groups, the relatively higher BL signal in the control group taurine + **FK-Luc-BH** was probably caused by the incomplete consumption of  $\text{ClO}^-$  by taurine in tumor cells. In addition, the systemic toxicities of BL probes were evaluated for each group after the last time point for imaging (120 min after the injection of **FK-Luc-BH** or **Ac-Luc-EA**). The mice were sacrificed before blood was collected from the eyeballs, then the major organs (heart, liver, spleen, lung, and kidney) and tumors were selected for hematoxylin–eosin (HE) staining. In contrast with the mice in the sham-operated group, which were only i.p. injected with PBS, the HE staining results revealed that no pathological changes were detected in all tissues mentioned above (Fig. S31†), indicating the good biocompatibility of the AND-gate BL probe **FK-Luc-BH**.

To prove the improvement of this novel AND-gate bioluminescent probe over the single-locked probes, 3  $\times$  10<sup>5</sup> 4T1-fluc cells were implanted separately into the second and fourth mammary fat pads of the 7-week-old Balb/c mice. When the tumors reached about 200 mm<sup>3</sup>, the mice were randomly divided into seven groups (*n* = 3) for comparing the BL properties of **FK-Luc-BH** and single-locked probes **Luc-BH** ( $\text{ClO}^-$ -responsive) and **FK-Luc** (CTS-responsive). Mice in the experimental group **FK-Luc-BH** were administered i.p. with 12.5  $\mu$ mol kg<sup>-1</sup> **FK-Luc-BH**, and the tumors around the second and fourth mammary fat pads are close to each other in the BL intensity (Fig. S32A and B†). However, for the control group taurine + **FK-Luc-BH** or the control group E-64d + **FK-Luc-BH**, when 12.5  $\mu$ mol kg<sup>-1</sup> **FK-Luc-BH** was injected i.p. after the intratumoral injection of 3 mmol kg<sup>-1</sup> taurine or 0.05 mmol kg<sup>-1</sup> E-64d into either of the tumors of each mouse, the BL signal of the tumors that were preinjected with taurine or E-64d was significantly lower than that of the other unpretreated ones (Fig. S32A, C and D†). These results further demonstrate that the BL “turn-on” of **FK-Luc-BH** requires both  $\text{ClO}^-$  and cathepsins, which will make this AND-gate probe more precise than the single-locked probes discussed below. To assess the BL properties of the single-locked probes **Luc-BH** and **FK-Luc**, after the intratumoral injection of 3 mmol kg<sup>-1</sup> taurine or 0.05 mmol kg<sup>-1</sup> E-64d into either of the tumors of each mouse, the mice were administered i.p. with **Luc-BH** or **FK-Luc** (12.5  $\mu$ mol kg<sup>-1</sup>), respectively. As shown in Fig. S33,† the BL intensity of **Luc-BH** was largely influenced by the level of  $\text{ClO}^-$  but not CTS, hence making it unable to differentiate the tumors with other  $\text{ClO}^-$ -related diseases, such as inflammation and neurodegenerative disorders.<sup>19,31–34</sup> Similarly, the BL intensity of **FK-Luc** only depends on the concentration of CTS (Fig. S34†), that may cause undesirable background signals and even false-positive results in other CTS-sufficient tissues, for example, the lung



**Fig. 4** Serial *in vivo* BLI of 4T1-fLuc tumor-bearing Balb/c mice after the intraperitoneal administration of  $12.5 \mu\text{mol kg}^{-1}$  FK-Luc-BH (the first row),  $12.5 \mu\text{mol kg}^{-1}$  Ac-Luc-EA (the second row), and  $12.5 \mu\text{mol kg}^{-1}$  FK-Luc-BH with the intraperitoneal pre-injection of  $3 \text{ mmol kg}^{-1}$  taurine for 5 min (the third row),  $0.05 \text{ mmol kg}^{-1}$  E-64d for 1 h (the fourth row), or both of them (the fifth row), respectively. The images were acquired at 10, 20, 40, 60, 80, 100 and 120 min after the injection of FK-Luc-BH or Ac-Luc-EA. Experiments were repeated independently three times in three mice with similar results. (B) Quantified total photon output using ImageJ software. (C) Quantified total photos of (B) at 20 min. Each error bar represents the standard deviation of the three independent experiments; the *p* value obtained from *t*-tests using comparisons of two groups (\*\* for *p* = 0.0038, \*\*\* for *p* = 0.0001, and \*\*\*\* for *p* < 0.0001).

and liver.<sup>35</sup> To further validate the good specificity of **FK-Luc-BH**, the Balb/c mice were randomly divided into three groups ( $n = 3$  for each group), and the mice in each group were intraperitoneally administered with  $12.5 \mu\text{mol kg}^{-1}$  **FK-Luc-BH**, **FK-Luc**, or **Luc-BH**. 40 min after injection, the Balb/c mice were sacrificed and their organs (hearts, lungs, livers, spleens, kidneys, and muscles) were harvested to prepare 15 wt% tissue homogenates. After the addition of  $0.1 \text{ mg mL}^{-1}$  fLuc,  $1 \text{ mM}$  ATP, and  $10 \text{ mM Mg}^{2+}$ , the BL signal of tissue homogenates was measured using a small animal imaging system. As shown in Fig. S35,† **FK-Luc-BH** showed a lower background BL signal in the tissues than **FK-Luc** and **Luc-BH**. All of the above results suggest that the dual-locked BL probe **FK-Luc-BH** shows lower background interference and better specificity compared with the single-locked probes for the imaging of tumors co-expressing  $\text{ClO}^-$  and CTSL.

## Conclusion

In conclusion, by caging the amino group of  $\text{NH}_2\text{-Luc}$  with the CTSL-recognizing substrate FK and the carboxyl group of  $\text{NH}_2\text{-Luc}$  with the  $\text{ClO}^-$  reactive motif benzoylhydrazine, an AND-gate BL probe **FK-Luc-BH** was designed for precise imaging of tumors where CTSL and  $\text{ClO}^-$  co-localized. *In vitro* experiments

indicated that **FK-Luc-BH** was able to efficiently convert to free  $\text{NH}_2\text{-Luc}$  when simultaneously incubated with CTSL and  $\text{ClO}^-$  and hence exhibited a bright BL signal after catalyzing by fLuc. The selectivity of **FK-Luc-BH** towards CTSL and  $\text{ClO}^-$  was evidenced by monitoring the BL responses of **FK-Luc-BH** to various biological species in solution. Cell experiments and animal experiments demonstrated that the coordination of CTSL and  $\text{ClO}^-$  enabled the BL signal of **FK-Luc-BH** to be significantly enhanced in 4T1-fLuc cells or 4T1-fLuc tumor sites, when compared with that of the unresponsive control compound **Ac-Luc-EA** group and the 4T1-fLuc cells or tumors that were co-treated with **FK-Luc-BH** with  $\text{ClO}^-$  scavenger taurine or/and broad-spectrum cathepsin inhibitor E-64d, suggesting the good specificity and accuracy of **FK-Luc-BH** for tumor imaging. By replacing the caging motifs for  $\text{NH}_2\text{-Luc}$  (*i.e.* FK and benzoylhydrazine in this work) with other responsive sites, this AND-gate platform can be employed for specifically imaging other diseases.

## Data availability

The ESI† includes all experimental details. General methods; syntheses and characterization studies of **FK-Luc-BH**, **Luc-BH** and **Ac-Luc-EA**.

## Author contributions

C. Wang performed syntheses, characterization, *in vitro* and *in vivo* experiments. Y. Hong, L. Dong, H. Chen and Z. Yu helped with characterization and cell experiments. D. Jin and R. Zhao helped with the construction of a 4T1-fLuc tumor bearing mouse model and *in vivo* experiments, respectively. Y. Yuan designed this project and wrote the paper. All the authors provided suggestions and comments on the manuscript.

## Conflicts of interest

There are no conflicts to declare.

## Acknowledgements

This work was supported by the National Key R&D Program of China (2022YFA1305100), the National Natural Science Foundation of China (22175168), the Collaborative Innovation Program of Hefei Science Center, CAS (2021HSC-CIP012), and the Fundamental Research Funds for the Central Universities (WK2060000020). For animal imaging, all animals received care according to the guidelines outlined in the Guide for the Care and Use of Laboratory Animals. The procedures were approved by the University of Science and Technology of China Animal Care and Use Committee (Permit Number: USTCACUC23010122026).

## References

- 1 J. C. Widen, M. Tholen, J. J. Yim, A. Antaris, K. M. Casey, S. Rogalla, A. Klaassen, J. Sorger and M. Bogyo, *Nat. Biomed. Eng.*, 2021, **5**, 264–277.
- 2 X. B. Zhao, J. Y. Kang and Y. P. Shi, *Anal. Chem.*, 2022, **94**, 6574–6581.
- 3 J. Chan, S. C. Dodani and C. J. Chang, *Nat. Chem.*, 2012, **4**, 973–984.
- 4 X. Wu, R. Wang, N. Kwon, H. Ma and J. Yoon, *Chem. Soc. Rev.*, 2022, **51**, 450–463.
- 5 Z. Qing, J. Xu, J. Hu, J. Zheng, L. He, Z. Zou, S. Yang, W. Tan and R. Yang, *Angew. Chem., Int. Ed.*, 2019, **58**, 11574–11585.
- 6 X. Zhao, Q. Han, N. Na and J. Ouyang, *Anal. Chem.*, 2021, **93**, 14514–14520.
- 7 L. Wu, A. C. Sedgwick, X. Sun, S. D. Bull, X. P. He and T. D. James, *Acc. Chem. Res.*, 2019, **52**, 2582–2597.
- 8 M. Yang, J. Fan, J. Du and X. Peng, *Chem. Sci.*, 2020, **11**, 5127–5141.
- 9 Q. Miao and K. Pu, *Adv. Mater.*, 2018, **30**, 1801778.
- 10 L. Wu, J. Huang, K. Pu and T. D. James, *Nat. Rev. Chem.*, 2021, **5**, 406–421.
- 11 A. P. de Sliva, N. H. Q. Gunaratne and C. P. McCoy, *Nature*, 1993, **364**, 42–44.
- 12 Y. Liu, L. Teng, C. Xu, H. W. Liu, S. Xu, H. Guo, L. Yuan and X. B. Zhang, *Chem. Sci.*, 2019, **10**, 10931–10936.
- 13 S. Chen, M. Chen, J. Yang, X. Zeng, Y. Zhou, S. Yang, R. Yang, Q. Yuan and J. Zheng, *Small*, 2021, **17**, 2100243.
- 14 L. Wu, H. H. Han, L. Liu, J. E. Gardiner, A. C. Sedgwick, C. Huang, S. D. Bull, X. P. He and T. D. James, *Chem. Commun.*, 2018, **54**, 11336–11339.
- 15 J. L. Kolanowski, F. Liu and E. J. New, *Chem. Soc. Rev.*, 2018, **47**, 195–208.
- 16 A. C. Love and J. A. Prescher, *Cell Chem. Biol.*, 2020, **27**, 904–920.
- 17 A. J. Syed and J. C. Anderson, *Chem. Soc. Rev.*, 2021, **50**, 5668–5705.
- 18 M. Verdoes, K. Oresic Bender, E. Segal, W. A. van der Linden, S. Syed, N. P. Withana, L. E. Sanman and M. Bogyo, *J. Am. Chem. Soc.*, 2013, **135**, 14726–14730.
- 19 Y. W. Yap, M. Whiteman and N. S. Cheung, *Cell. Signalling*, 2007, **19**, 219–228.
- 20 A. Daugherty, J. L. Dunn, D. L. Rateri and J. W. Heinecke, *J. Clin. Invest.*, 1994, **94**, 437–444.
- 21 S. M. Wu and S. V. Pizzo, *Arch. Biochem. Biophys.*, 2001, **391**, 119–126.
- 22 S. Weitzman and L. Gordon, *Blood*, 1990, **76**, 655–663.
- 23 S. R. Mullins, M. Sameni, G. Blum, M. Bogyo, B. F. Sloane and K. Moin, *Biol. Chem.*, 2012, **393**, 1405–1416.
- 24 M. Assi, *Am. J. Physiol.: Regul., Integr. Comp. Physiol.*, 2017, **313**, 646–653.
- 25 J. Huang, X. Chen, Y. Jiang, C. Zhang, S. He, H. Wang and K. Pu, *Nat. Mater.*, 2022, **21**, 598–607.
- 26 B. Hu, N. Song, Y. Cao, M. Li, X. Liu, Z. Zhou, L. Shi and Z. Yu, *J. Am. Chem. Soc.*, 2021, **143**, 13854–13864.
- 27 H. Li, Q. Yao, F. Xu, Y. Li, D. Kim, J. Chung, G. Baek, X. Wu, P. Hillman, E. Lee, H. Ge, J. Fan, J. Wang, S. Nam, X. Peng and J. Yoon, *Angew. Chem., Int. Ed.*, 2020, **59**, 10186–10195.
- 28 L. Zhu, H. W. Liu, Y. Yang, X. X. Hu, K. Li, S. Xu, J. B. Li, G. Ke and X. B. Zhang, *Anal. Chem.*, 2019, **91**, 9682–9689.
- 29 J. Liu, S. Zhang, B. Zhao, C. Shen, X. Zhang and G. Yang, *Biosens. Bioelectron.*, 2019, **142**, 111497.
- 30 D. Ma, Q. Zong, Y. Du, F. Yu, X. Xiao, R. Sun, Y. Guo, X. Wei and Y. Yuan, *Acta Biomater.*, 2021, **135**, 628–637.
- 31 H. Feng, Z. Zhang, Q. Meng, H. Jia, Y. Wang and R. Zhang, *Adv. Sci.*, 2018, **5**, 1800397.
- 32 C. Ma, S. Hou, X. Zhou, Z. Wang and J. Yoon, *Anal. Chem.*, 2021, **93**, 9640–9646.
- 33 T. M. Jeitner, M. Kalogiannis, B. F. Krasnikov, I. Gomolin, M. R. Peltier and G. R. Moran, *Toxicol. Sci.*, 2016, **151**, 388–402.
- 34 C. Yin, H. Zhu, C. Xie, L. Zhang, P. Chen, Q. Fan, W. Huang and K. Pu, *Adv. Funct. Mater.*, 2017, **27**, 1700493.
- 35 Y. Huang, S. Li, S. Huang, J. Tu, X. Chen, L. Xiao, B. Liu and X. Yuan, *Front. Bioeng. Biotechnol.*, 2022, **10**, 780751.

